

The role of myocardial wall thickness in atrial arrhythmogenesis

John Whitaker^{1*}, Ronak Rajani², Henry Chubb^{1,3}, Mark Gabrawi¹, Marta Varela¹, Matthew Wright¹, Steven Niederer¹, and Mark D. O'Neill¹

¹Electrophysiology Division of Cardiovascular Directorate and Division of Imaging Sciences and Biomedical Engineering, King's College London, 4th Floor, North Wing, St Thomas' Hospital, Westminster Bridge Road, London SE1 7EH, UK; ²Department of Cardiac Computed Tomography, Cardiovascular Directorate, Guy's and St Thomas NHS Foundation Trust, London, UK; and ³Department of Paediatric Cardiology, Evelina London Children's Hospital, London, UK

Received 11 November 2015; accepted after revision 13 January 2016; online publish-ahead-of-print 31 May 2016

Changes in the structure and electrical behaviour of the left atrium are known to occur with conditions that predispose to atrial fibrillation (AF) and in response to prolonged periods of AF. We review the evidence that changes in myocardial thickness in the left atrium are an important part of this pathological remodelling process. Autopsy studies have demonstrated changes in the thickness of the atrial wall between patients with different clinical histories. Comparison of the reported tissue dimensions from pathological studies provides an indication of normal ranges for atrial wall thickness. Imaging studies, most commonly done using cardiac computed tomography, have demonstrated that these changes may be identified non-invasively. Experimental evidence using isolated tissue preparations, animal models of AF, and computer simulations proves that the three-dimensional tissue structure will be an important determinant of the electrical behaviour of atrial tissue. Accurately identifying the thickness of the atrial may have an important role in the non-invasive assessment of atrial structure. In combination with atrial tissue characterization, a comprehensive assessment of the atrial dimensions may allow prediction of atrial electrophysiological behaviour and in the future, guide radiofrequency delivery in regions based on their tissue thickness.

Keywords Left atrial wall thickness • Atrial fibrillation • AF • Cardiac computed tomography • Cardiac CT

Introduction

Changes in the structure and electrical behaviour of the left atrium are known to occur with conditions that predispose to atrial fibrillation (AF) and in response to prolonged periods of AF. The temporal progression, as well as the relative importance of, structural and electrical remodelling remains obscure and is likely to vary among patients with AF. The human left atrial (LA) wall is a thin structure, which has made it difficult to assess *in vivo* until recently. Traditional assessment of the LA has been restricted to chamber size and flow measurement; however, as technology and experience with high-resolution cross-sectional imaging techniques have improved, the accurate assessment of the atrial wall has become a realistic prospect. Although AF can be effectively treated with radiofrequency catheter ablation (RFCA), for some groups outcomes remain suboptimal. The identification of structural parameters that may optimize patient selection and refine treatment delivery has therefore assumed greater importance. We review the published data regarding the thickness of the left atrial wall (LAWT) in pathological specimens and from imaging studies. We discuss the evidence

that LAWT is a parameter that varies with clinical status, the potential for its use as a marker for pathological atrial remodelling and the evolving evidence emphasizing the importance of the three-dimensional structure of the atrial wall in arrhythmogenesis. Finally, we consider the role of LAWT in predicting the response to invasive treatment of AF and its potential for improving the safety of RFCA procedures.

Atrial wall thickness: pathological assessment and effect of cardiovascular comorbidities

Direct examination of atrial tissue in the *ex vivo* state has provided valuable information about atrial structure. Left atrial wall thickness has been systematically measured in a number of post-mortem studies, which are summarized in *Table 1*. The left atrium is a thin-walled structure whose shape and volume is likely to be highly sensitive to changes in loading conditions. This is relevant to any conclusions drawn about LA shape and wall thickness drawn from specimens

* Corresponding author. Tel: +44 2 07 1887188 ext. 56308; fax: +44 2 07 1885442. E-mail address: john.whitaker@kcl.ac.uk

Published on behalf of the European Society of Cardiology. All rights reserved. © The Author 2016. For permissions please email: journals.permissions@oup.com.

Table 1 Pathological studies of left atrial wall characteristics

Year	Author	Number of specimens	Age range of specimens	Co-morbidities	Methods of preparation	Methods of examination	Sites examined	Measured parameter	Measurements/mm	Outcome
1995	Wang et al. ³³	9	NR	NR	Fixed 10% formalin 1 week	NR	NR	LA wall thickness	Range 3–5	
1999	Ho et al. ⁶	26	25–85 (mean 52 ± 18)	Bl	Fixed in 10% formalin	NR	<ul style="list-style-type: none"> Anterior wall (Ant) Posterior wall (Post) Superior wall (Sup) Lateral wall (Lat) Vestibule (Vest) (No further details regarding location sampled) 	LA wall thickness in each location	Site Ant 3.3 ± 2.1 Post 4.1 ± 0.7 Sup 4.5 ± 0.6 Lat 3.9 ± 0.7 Vest 2.3 ± 0.7 Range 1.5–4.8 2.5–5.3 3.5–6.5 2.5–4.9 1.2–3.3	
2003	Hassink et al. ⁷⁵	20	46–88	CV, NCV, AF	Specimens measured freshly at autopsy (and subsequent histology on formalin-fixed samples)	NR	<ul style="list-style-type: none"> PV ostia Anterior wall midway between PV ostia Posterior wall between PV ostia 	Site Anterior wall 1.6 ± 0.5 mm Posterior wall 1.7 ± 0.6 mm Range 1.0–2.5 mm 1.1–2.6 mm	Mean ± SE 1.6 ± 0.5 mm 1.7 ± 0.6 mm Range 1.0–2.5 mm 1.1–2.6 mm	Variable extension of atrial myocardium into PV sleeves, which was greater in patients with AF. Hypertrophy, fibrosis, and disorganization greater in PV myocardium of AF patients
2004	Becker ¹	20	27–93 (mean 63.5)	NCV, CV, CM, NCM	Through and through incision from left inferior pulmonary vein os to mitral valve annulus (shortest distance)—corresponding to mitral isthmus	Caliper on gross specimen	<ul style="list-style-type: none"> Immediately below LIPV os (PV) Midway between LIPV and MV (Mid) Directly above MV annulus (MV) 	Myocardial thickness	Site PV 3.0 Mid 2.8 MV 1.2 Range 1.4–7.7 1.2–4.4 0–3.2	In addition, atrial myocardium extends onto the atrial aspect of MV leaflet
2005	Sanchez-Quintana et al. ³	30	Mean 54 ± 12	CV, NCV	Isolated heart lung blocks fixed in 10% buffered formalin, sectioned in sagittal planes at regions: left VA junction, middle of posterior atrial wall, and right VA junction	Caliper on prepared sections	<ul style="list-style-type: none"> Posterior LA wall - superior (sup), middle (mid) and inferior (inf) portions in three different planes—left veno-atrial (VA) junction, middle of posterior wall (MidP) and right VA junction 	Transmural thickness at these locations Myocardial thickness in addition (not included in table)	Site RVA Sup 2.3 ± 0.5 MidP Sup 2.5 ± 0.5 LVA Sup 2.2 ± 0.3 RVA Mid 2.8 ± 0.5 MidP Mid 3.8 ± 0.6 LVA Mid 3.5 ± 1.2 RVA Inf 5.7 ± 2.5 MidP Inf 6.5 ± 2.5 LVA Inf 5.3 ± 2.0 Range 1.1–4.8 1.1–5.3 1.2–4.5 1.5–5.0 3.1–5.0 1.7–5.0 2.7–10.0 2.8–12.0 2.5–9.0	
2005	Deneke et al. ⁷⁶	7	61–76	All AF post-ablation	Tissue staining of paraffin blocks taken at autopsy	Direct measurement of tissue blocks	<ul style="list-style-type: none"> Left atrial isthmus Pulmonary vein ostia Posterior LA wall 	Transmural thickness Percentage of wall ablated	Wall thickness range LA isthmus 4–10 mm PV ostia 1–3 mm Posterior LA wall 2–5 mm	

Continued

Table 1 Continued

Year	Author	Number of specimens	Age range of specimens	Co-morbidities	Methods of preparation	Methods of examination	Sites examined	Measured parameter	Measurements/mm	Outcome
2006	Hall et al. ²	34	NR	CV, NCV, CM, NCM, AA	Fixed in 10% formalin, bisected along the sagittal plane and parallel incisions made	Caliper on prepared specimens	<ul style="list-style-type: none"> Anterior (ant) Roof (between superior aspect of right and left PV) Posterior wall (post) Mitral isthmus (MI) (MI)/(between LIPV and mitral annulus) Interatrial septum (IAS) 	Transmural thickness	Mean \pm SD 1.86 \pm 0.59 1.06 \pm 0.49 1.4 \pm 0.46 1.6 \pm 0.48 2.2 \pm 0.82	Sig differences between thickness of roof compared with other areas, post wall sig thinner than sept, ant and lsh, sept thickest sig thicker than other regions
2008	Cabrera et al. ⁴	40	Mean 49 \pm 20 years	CV, NCV, AA	LA walls dissected to display lateral region LA between roof of atrium, left PVs and MV. Blocks of tissue encompassing left PVs, LLR, LAA, mitral vestibule and annulus serially sectioned at 12 or 15 μ m in sagittal ¹³ or frontal ¹ planes. Masson's trichrome stain at 1 mm intervals	Caliper on gross specimens and then on ²² histological specimens	<ul style="list-style-type: none"> LLR—on lateral LA wall between ostia of left PVs and CS os, at superior (sup) and inferior (inf) level. Measurements taken perpendicular to endocardium in both macroscopic and histologic specimens 	Myocardial thickness at superior level Myocardial thickness at inferior level	Mean \pm SD 2.8 \pm 1.1 1.7 \pm 0.8 1.5–4.2 0.5–3.5	
2008	Platonov et al. ⁵	298	Mean age 61 \pm 17	AF, no AF	'Routine autopsy' on fresh specimens, not fixed in formalin	Calipers to measure transmural thickness excluding fat	<ul style="list-style-type: none"> Posterior wall—3 sites—midway between superior PV ostia, middle of all four PV ostia and between inferior PV ostia. Total range 1–8 mm across all sites 	Superior pulmonary veins (SPV) Centre of four pulmonary veins (CPV) Inferior pulmonary veins (IPV)	Mean \pm SD (no AF group) 2.3 \pm 1.0 2.6 \pm 1.0 2.9 \pm 1.3 3.1 \pm 1.3 3.2 \pm 1.4 3.1 \pm 1.5 4.6 \pm 1.2	Mean \pm SD (AF group) 2.1 \pm 0.9 2.2 \pm 1.0 2.5 \pm 1.3 3.1 \pm 1.3 3.2 \pm 1.4 3.1 \pm 1.5 4.6 \pm 1.2
2009	Wolf et al. ⁸	53 (47 Fontan and 8 controls)	Fontan: 7.7 \pm 9.2 Control: age <21	Fontan group Control group: NCD	Fixed in 10% formalin	NR (Masson trichrome formalin-fixed sections for fibrosis analysis)	<ul style="list-style-type: none"> Three different free wall sites: superior, lateral, and inferior—mean calculated on the basis of this 	Fontan transmural thickness Control transmural thickness	Mean \pm SD 1.8 \pm 0.5 2.3 \pm 0.6	Significant difference in LAVWT between Fontan and control groups
2013	Schwartzman et al. ⁷	15	0–69	NCV, (incidental discovery of SCV changes in 2)	Transmural sections of fresh cardiac tissue. LM: specimens fixed in formalin and embedded in paraffin blocks. Stained with Haematoxylin and Eosin, Trichrome and Verhoeff-Van Gieson stains EM: ultrathin sections (60 nm) and stained in 4% uranyl-acetate and 1% lead citrate—transmission electron microscopy	Calipers on light microscopy sections	<ul style="list-style-type: none"> Atrial body—including low posterior wall (low post), middle posterior wall (mid post), roof and septum (IAS) appear to be areas 	Transmural thickness 'Atrial intimal thickness' (AIT) (values not included)	Mean \pm /SD	Demonstrated significant difference in AIT between age groups

NR, not reported; B, blinded; NCV, patients without a history of cardiovascular disease (excluding atrial arrhythmias); AA, history of atrial arrhythmias; CM, significant (non-cardiac) co-morbidities; NCM, no significant co-morbidities; SCV, structural cardiovascular changes seen at autopsy; NCD, died from non-cardiac disease.

examined in the *ex vivo* state. The tissue fixing process represents a potential source of error when attempting to establish the LA structure in the thorax from tissue specimens.

There is significant variation in LAWV between patients when considered in pathological studies. The majority of studies report average measurements of wall thickness between 1 and 4 mm^{1–4} with a range of reported measurements extending between 0.5⁴ and 12 mm.³ Regional differences in atrial wall thickness are consistently identified in these studies. There is agreement among the tissue-based studies that the posterior wall thickness increases when moving from the superior aspect to the inferior aspect.^{3,5} Different conclusions are reached regarding comparative tissue thickness between the anterior and posterior wall.^{2,6} In addition to changes in wall thickness, an age-related increase in LA intimal thickness, fibrosis, and disorganization has been identified in pathological specimens of human atria.⁷

A group of pathological studies have compared LAWV measurements between groups of patients with different clinical profiles. Wolf *et al.*⁸ compared post-mortem atrial wall thickness in young patients who had undergone Fontan procedure palliation for uni-ventricular physiology with controls who had died from non-cardiac disease. As expected the right atrium was significantly thicker in those treated with Fontan procedure. The mean LAWV was also 0.5 mm thicker in the Fontan group than in the control group. In the largest cohort of measurements of LAWV reported in a tissue-based study, Platonov *et al.*⁵ considered the posterior LA wall in 298 consecutive pathological specimens at routine autopsy. In this study, the posterior LA wall was significantly thinner in patients with a history of AF when compared with those without a history of AF. In this study, the mean posterior wall thickness was 2.6 and 2.9 mm, respectively, in the middle and inferior portion of the posterior wall in the no-AF group, and 0.4 mm lower at each level in the AF group.⁵

While atrial remodelling occurring in response to changes in atrial pressures resulting in increased atrial wall thickness in the context of a Fontan circulation is a plausible and likely sequence of events, establishing the temporal relationship between atrial structural changes and the development of atrial arrhythmias is more challenging. Structural changes (including changes in atrial wall thickness) are likely to result from pathological remodelling in response to altered haemodynamics occurring in conditions that predispose to AF. In addition, atrial structural remodelling is known to occur with prolonged episodes of AF⁹ itself and this may include changes in LAWV. Myocyte hypertrophy is seen in many different animal models of AF.¹⁰ Regardless of the temporal sequence of events, it is possible that if it could be assessed non-invasively, atrial wall thickness could become a useful marker of atrial pathological remodelling in patients at risk of, or already diagnosed with, AF.

Non-invasive assessment of left atrial wall thickness

Until recently, echocardiography was the only widely available tool available for cardiac structural assessment in AF patients. A very large evidence base has been collected that comprehensively demonstrates the value of echocardiographic atrial assessment. Two-dimensional estimates of atrial size were traditionally used to

measure and follow atrial dilatation, and robust follow-up data document the value of this as a measure of atrial remodelling that has been shown independently predict progression of AF.¹¹ Novel echocardiographic markers¹² add additional value, and Doppler techniques allow non-invasive assessment of transmitral flow.¹³ These features will ensure that echocardiography remains a key part of the imaging assessment of AF patients. Despite these strengths, at present echocardiography is not well suited to the assessment of atrial tissue thickness. Transthoracic echocardiography does not routinely provide adequate spatial resolution to allow assessment of LAWV, although it has been reported for this indication.¹⁴ Transesophageal echocardiography (TEE) or intracardiac echocardiography (ICE) provides the highest spatial resolution. Transesophageal echocardiography was used to identify an increase in the interatrial septum thickness (IAST) in patients with a history of AF.¹⁵ Intracardiac echocardiography (with a maximum spatial resolution of 0.2–0.3 mm) has been demonstrated to accurately assess changes in right atrial wall thickness following application of radio-frequency (RF) energy in an experimental model.¹⁶ Changes in wall thickness were also demonstrated to correlate with depth of lesion formation. The invasive nature of these investigations and the limited extent of atria TEE can image¹⁷ means that in general these investigations have been limited to the peri-procedural period where their value is clearly established.

Cardiac magnetic resonance (CMR) imaging has emerged as the optimal modality for myocardial tissue characterization. Ventricular imaging using CMR is now acknowledged as the gold standard for the identification and localization of scar¹⁸ as well as for the assessment of ventricular function. More recently, atrial myocardial imaging has expanded and it now has a key role in the assessment of patients with atrial arrhythmias. Cardiac magnetic resonance has been used to identify pathological atrial remodelling through the identification of fibrosis.¹⁹ Accumulating evidence suggests that this may be useful in the prediction of disease progression. Cardiac magnetic resonance has been used in animal models²⁰ and clinical studies²¹ to identify RF lesions. In some centres, CMR has been used to identify gaps in lesions to guide further invasive treatment of AF.²² Novel indices of atrial remodelling including shape assessment may offer additional value in prediction of response to invasive treatment of AF.^{23,24} Cardiac magnetic resonance will remain a critical tool for atrial assessment in pre- and post-ablation patients. The most effective way to harness the power of CMR to assess different groups of AF patients continues to be refined, tested, and debated.^{25,26} Cardiac magnetic resonance has been used in a small number of studies to assess LAWV. Hsing *et al.*²⁷ measured LAWV at a single atrial site and demonstrated an increase in LAWV of around 4 mm following application of RF energy at a single site in the left atrium. In addition, Yokokawa *et al.*²⁸ report that the magnitude of change in LAWV following application of RF energy at discrete anatomical sites is a predictor of early recurrence of AF. The mean measured wall thickness prior to application of RF energy in Hsing *et al.*'s study was 7 mm, a greater value than reported in the majority of pathological studies and other imaging studies. This is likely to reflect an averaging effect seen in which the spatial resolution of the imaging technique is below that of the structure being imaged ('partial volume effect'). While CMR is the optimal modality for atrial tissue characterization, the ability of CMR to precisely

identify atrial wall thickness in this case may be limited by the spatial resolution of currently available commercial CMR systems.

Computed tomography (CT) has emerged as the optimal modality for assessing the LA wall and, in addition, provides information about LA structure and shape under *in vivo* loading conditions. A number of studies have used cardiac CT to assess LAWT and these are summarized in Table 2.

In the first study to measure atrial wall thickness using cardiac CT, Lemola *et al.*²⁹ took measurements of the thickness of the posterior LA wall at three different levels. In contrast to pathological studies, no significant differences in the LAWT at the superior, middle, and inferior level were identified. Hoffmeister *et al.*³⁰ report a mean LAWT of 2.4 ± 0.5 mm without further details of the measurement locations, the method of defining the boundaries of the wall, or the orientation chosen for the measurement. Beinhart *et al.*³¹ examined CT scans from consecutive patients undergoing persistent AF ablation and recorded LAWT measurements from 12 pre-determined locations. Measurement was taken at the thickest measurable muscular segments and demonstrated significant inter- and intra-patient variability in LAWT measurements. When viewed alongside the results of tissue studies from similar locations, the CT measurements are generally lower than the tissue measurements.^{1,3-7}

Association between left atrial wall thickness and clinical characteristics

Left atrial wall thickness has been demonstrated to increase between the ages of 50 and 79.³² In the same study, Pan *et al.*³² also observed the anterior LAWT was significantly greater than posterior LAWT in 180 patients without coronary or other known cardiac disease. These results are consistent with those results from several pathological studies^{2,33} while discrepant with the results from Ho *et al.*⁶

Imada *et al.*³⁴ did not identify a significant difference between measurements of atrial wall thickness taken from the anterior wall between patients with paroxysmal AF (PAF) and non-PAF. In this study, the mean LAWT was 2.6 mm in both groups. Nakamura *et al.*³⁵ found that the anterior LAWT was significantly thicker in patients with PAF (LAWT 2.4 ± 0.2 mm) when compared with both a group with no history of AF (LAWT 1.9 ± 0.2 mm) and a group with non-PAF (LAWT 2.1 ± 0.2 mm). This CT-based study indicates that LAWT is a variable that may change with the presence of type of AF. The identification of an increase in anterior LAWT with PAF that regresses with the transition to persistent AF is of great interest, suggesting a complex progression of changes in atrial anatomy in parallel with well-documented atrial dilatation (Figures 1 and 2).³⁶

With the exception of a single tissue-based study, measurements of LAWT taken on CT are lower than those reported from *ex vivo* tissue samples.^{1,3-6} This may relate to the different loading conditions of the atria in the *in vivo* state when compared with the *ex vivo* state. It is also possible that there is a systematic underestimation of LAWT by CT. Computed tomography studies have not demonstrated the variation in LAWT seen at the different levels of the posterior wall that has been reported in pathological studies. It is not clear whether the variation in the posterior LAWT measured on pathological specimens reflects a change in atrial geometry between the *in vivo* and the *ex vivo* state, and is therefore an artefact

from preparation of the tissue samples, or whether this represents an insensitivity of the imaging modality to identify this variation.

An important challenge in CT assessment of LAWT is the accurate identification of the epicardial and endocardial surfaces. This is an inherent limitation of the imaging modality as a result of the low tissue contrast at the epicardial boundary. In CT imaging, the Hounsfield unit (HU) intensity is used to discriminate between the tissue types. In some areas, the atrial wall will have similar HU intensity to neighbouring structures (e.g. the aortic wall and the oesophagus), which will make accurate identification of the epicardial surface challenging. There is no consensus on the optimal method for identifying the borders between which measurements are taken. As more experience is gained, it seems likely that there will be increased use of automated algorithms for assessing these boundaries, as has been seen in the most recent studies.^{37,38} In addition, all studies so far have assessed LAWT in a single dimension at a discrete number of locations and extrapolated these measurements as representative of either regional or global LAWT. Given the anatomical complexity of the LA, it may be helpful to exploit the full data set available in order to make an assessment of LAWT. A novel method designed to make a three-dimensional assessment of LAWT that has been validated in a LA phantom has recently been reported.³⁹ Following identification of the epicardial and endocardial borders, non-intersecting field lines are derived between the two surfaces. This allows perpendicular measurements to be automatically calculated between these field lines, which provides wall thickness measurements throughout the atrium. If validated in a clinical setting, a global LAWT assessment will offer more detailed, accurate, and reproducible measurements to be identified from current imaging as well as offering the potential to derive estimates of atrial tissue mass.

Effect of atrial wall thickness on atrial electrophysiology

The 'critical mass hypothesis' was originally proposed in 1914⁴⁰ as one of several early theories to explain the pattern of electrical activity responsible for AF. Although in the intervening decades our understanding of AF has progressed, many contemporary models of the electrical patterns required to sustain fibrillation in atrial tissue also depend upon a critical mass of tissue being present, whether they depend upon the propagation of multiple wavelets⁴¹⁻⁴⁴ or the existence of localized focal re-entrant mechanisms driving AF.⁴⁵⁻⁴⁸

Experimental evidence in support of a critical mass of atrial tissue being required to sustain AF comes from Byrd *et al.*⁴⁹ and Lee *et al.*⁵⁰ who demonstrated that the size of tissue sections correlated with the probability of being able to induce sustained AF within the sections. These data are in keeping with the progressive atrial dilatation seen over time with AF, and its reconciliation with the long-held observation that 'AF begets AF'.⁵¹

In addition to simple quantification of atrial mass impacting upon the ability of atrial tissue to sustain arrhythmias, investigators have considered the impact of the complex atrial architecture upon the electrophysiological mechanisms involved in atrial arrhythmias. Using high-density simultaneous electrode mapping of the epicardial and endocardial surface of the right atrium in isolated perfused canine myocardium, Schuessler *et al.*⁵² demonstrated differences in

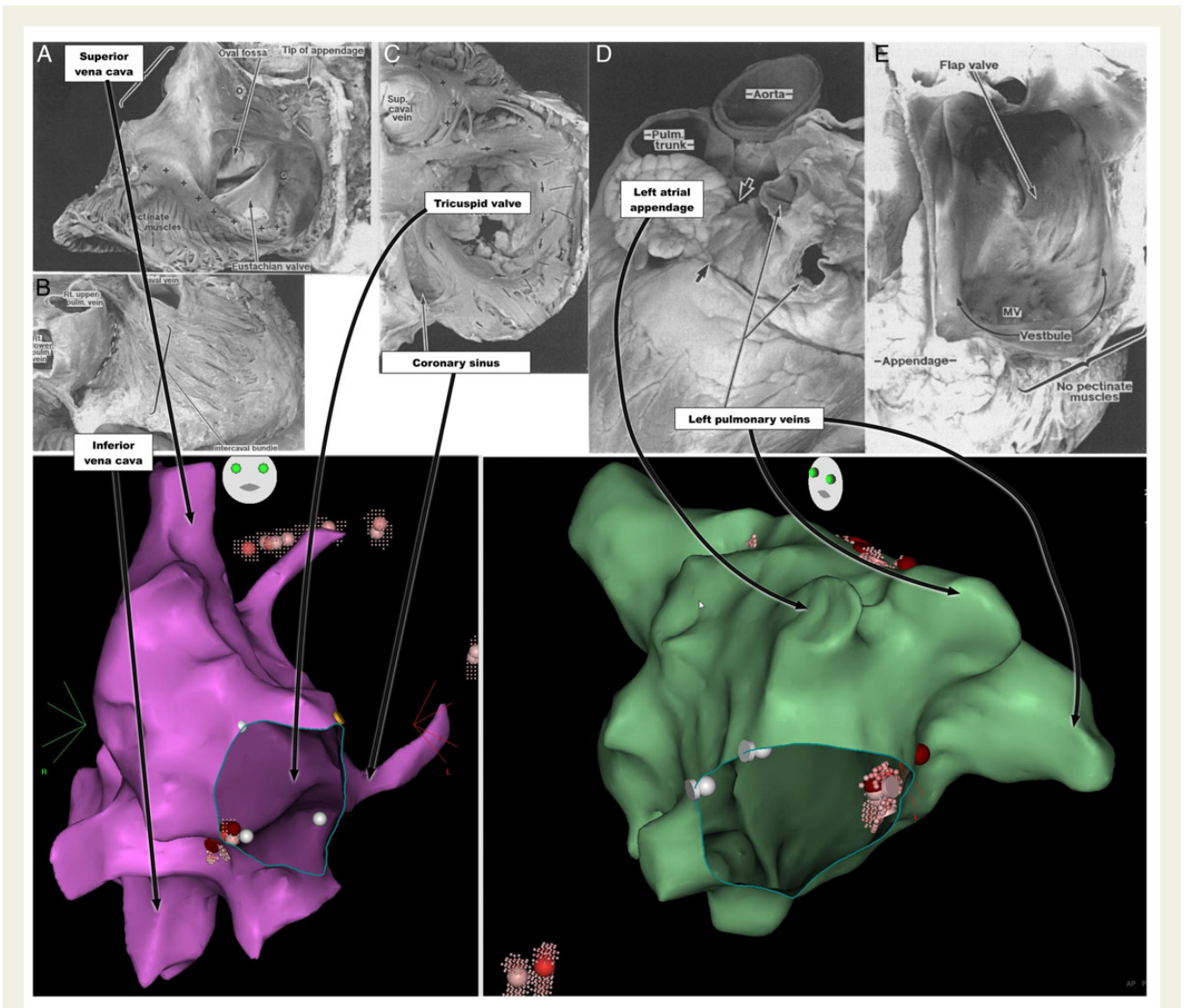


Figure 1 Human atrial anatomy: pathological specimens with corresponding anatomical landmarks from Carto electro-anatomical map of right atrium under anteroposterior projection (purple) and left atrium under modified left anterior oblique projection (green). (A–E) Reproduced with permission of *BMJ* publishing group from Wang *et al.*³³ (A) Right atrium opened through an incision that passes parallel to the right coronary artery to the tip of the appendage and then through the terminal crest (O–O) into the superior vena cava. Pectinate muscles arise along the length of the terminal crest (+ +) towards the coronary sinus (*). There is a prominent Eustachian valve in this specimen. (B) Atria viewed from behind showing intercalated bundle after pericardium removed. (C) Tricuspid valve viewed from the right atrium with the endocardium removed to reveal the internal circumferential bundle (arrows) encircling the vestibule. The pectinate muscles (lines) are perpendicular to the circumferential bundle. '+' indicates terminal crest. (D) External view of left atrium showing tubular appendage with arrow junction to pulmonary veins. (E) Internal aspect of left atrium demonstrating fossa ovalis on the septum. Pectinate muscles are confined to the appendage. The vestibule leading to the mitral valve (MV) is smooth.

the timing of activation between the two surfaces. In addition, the voltage amplitude of the signals measured corresponded to the atrial tissue thickness. Finally, they demonstrated that the atrial wall is capable of harbouring re-entrant circuits that exist between the epicardial and endocardial surface, rather than existing on one or the other surface as had previously been modelled. Everett *et al.*⁵³ measured the endocardial and epicardial activation sequences of experimental AF in five different canine models of AF. This study also

demonstrated transmural differences in activation pattern seen independently in each model,⁵³ providing further confirmation of the transmural patterns of electrical activation seen in fibrillating atria.

In Langendorf-perfused sheep hearts, Klos *et al.*⁵⁴ further characterized the effect of tissue structure in experimentally induced AF. They identified abrupt changes in the myocardial thickness and changes in muscle fibre orientation as being the key structural

Table 2 Studies in which computed tomography has been used to assess left atrial wall thickness

Year	Author	No of patients/CM	Spatial resolution	Method of measuring LAWT	Sampling of measurements of LAWT	Measurements	Histological studies of similar regions	Correlation with histological studies	Notes
2004	Lemola et al. ²⁹	50/all with AA (45pAF; 5 PsAF); NCV and CV	0.58 mm in all three dimensions	Digital calipers to measure distance from contrast filled LA to fat pad (identified by a change in signal density). Not reported how many measurements were taken or how they chose points to measure	Superior, middle, and inferior portions of LA posterior wall	Mean post LA wall thickness 2.2 ± 0.9 mm (range 0.9–7.4 mm)	2 4 5	2—CT gives lower measurement 4—CT gives similar result at superior level, lower measurement at middle and inferior level and does not identify the variation seen on tissue sample 5—CT gives higher measurement	
2007	Imada et al. ³⁴	33 (16PsAF, 17pAF)/ NCV and CV. Median age 68(PsAF) /62(pAF)	0.625 or 1.25 mm slice thickness	Single measurement on anterior LA wall measured from left sagittal view. Method of measurement not reported	Single measurement taken, location of this measurement not reported	Mean anterior LAWT 2.6 mm (SD and range not given)	2	2—CT gives lower measurement than histology	Also demonstrated neg correlation LAWT and LA diameter in PsAF only
2007	Hoffmeister et al. ³⁰	42 (26pAF, 16 no AA)	1 mm slice thickness	No details about method of measuring LAWT	No details	Mean LAWT 2.4 ± 0.5 mm	Not comparable		
2008	Pan et al. ³²	180 NCV	Not reported	No details about method for measuring LAWT	Anterior and posterior LAWT on axial slices. No details about level or number of measurements (mean ± SD)	Age Ant LAWT Post LAWT Difference	2 4 5	2—CT identifies anterior LAWT as greater than posterior LAWT in contrast to pathological study. Posterior wall measurements are lower by CT than histology, anterior wall measurements are similar to those found at histology 4—CT gives lower measurements than those found at histology 5—Posterior wall measurements similar, CT gives higher measurements for anterior wall 7—CT gives lower measurements for post LAWT	Change in LAWT with age Difference between ant and post LAWT Agree with Schwartzman et al. (number 8) in that age-related changes in the atrium are identified
2011	Nakamura et al. ³⁵	186 (62 each no AA, recurrent pAF, CAF)	1.25 mm (16 slice) or 0.625 mm (64 slice)	No report on how measurements were made (assume manually). Measurements taken on multiplanar reconstruction of section perpendicular to anterior LA wall	Anterior LA wall at level where anterior LA wall and aorta separate—given as mean value	Group CAF PAF No AA	2	2—CT gives lower measurement than histology in each group	Demonstrated pAF group had thicker anterior LAWT than no AA/CAF groups

Year	Author	Study Design	Sample Size	Measurement	Site	Mean ± SD	Range	Notes	Significance	
2011	Beinart et al. ³¹	60 (all AA—P _{SAF})	0.6 or 0.75 mm slice thickness	12 pre-selected locations. Thickest measurable muscular segment (fat excluded on basis of HU) within 5 mm of reference point	3 points on roof, 4 points on posterior wall, 3 points on floor, LLR and mitral isthmus origin	Roof right	2.03 ± 0.53	0.90–3.00	2—CT gives lower measurement than histology [PW/roof (listed as 'superior' wall in Ho et al)], other locations not obviously comparable 3—CT gives lower measurement at LLR than histology (taken representative) measurement in Becker paper as middle measurement 4—CT gives lower measurements than histology on right, mid, and left sections [compare floor measurements (8, 9, 10 on Beinart paper) with mid PW measurements of Sanchez-Quintana] 5—CT gives higher measurement than histology at roof (middle), lower measurement on PW (middle), higher measurement on isthmus 6—CT gives lower measurement than histology (superior level) 7—CT gives lower measurement [compare mid sup PW (region 5) with SPV] on sup PW than histology (both AF and no AF groups), mid PW (AF/no AF groups) 8—CT gives lower measurements than histology at sup PW (region 5 with region 7), mid PW (6 with 6), low PW (9 with 5)	Sig inter- and intra-patient variability in LAWT
						Roof middle	2.15 ± 0.47	1.190–3.30		
						Roof left	2.00 ± 0.46	1.00–2.80		
						Right PW	1.94 ± 0.55	0.90–3.00		
						Mid sup PW	1.43 ± 0.44	0.70–2.60		
						Mid PW	1.87 ± 0.45	0.80–3.10		
						Left PW	1.80 ± 0.42	0.70–2.80		
						Right floor	1.78 ± 0.49	0.70–2.60		
						Mid floor	1.81 ± 0.44	1.00–3.00		
						Left floor	1.74 ± 0.42	1.00–2.70		
						LLR	2.10 ± 0.63	0.50–3.50		
						MI	2.05 ± 0.47	0.90–2.80		
2013	Suenari et al. ⁶⁵	54 (all undergoing AF ablation) (inc CV, NCV, CM, NCM)	0.8 mm slice thickness at 0.4 mm intervals	No report on definition of wall borders, but measurements taken at middle of LA region on each sagittal section according to text (NB images show measurements on multipanar reconstructions)	Superior LLR (Sup LLR), inferior left lateral ridge (Inf LLR) Bottom of LA Posterior wall Roof LA Also measured PV antra and carina	AF recurrence group—mean ± SD	No AF recurrence group—mean ± SD	6	Demonstrated fusion of CT and EAMS Demonstrated sup LLR thickness correlated with AF recurrence	
						4.20 ± 1.08	5.58 ± 1.67			
					Sup LLR	4.25 ± 1.09	5.06 ± 1.52			

Continued

Table 2 Continued

Year	Author	No of patients/CM undergoing ablation	Spatial resolution	Method of measuring LAWT	Sampling of measurements of LAWT	Measurements	Histological studies of similar regions	Correlation with histological studies	Notes
2013	Dewland et al. ³⁸	187 (98 AA and 89 no AA)	1.25 mm slice thickness	Measurements in axial plane using an automated algorithm (validated on carotid CT). Algorithm required borders of contrasting density. After all slices from a given region compared thinnest measurement was recorded. Note: imaging for AF at random time in cardiac cycle, just prior to atrial systole in control	Interatrial septum, below RIPV, LAA, ant LA wall; thinnest LAWT measured	AF Control 0.7 mm (no range/SD) 0.9 mm (no range/SD)	Nil	No directly comparable regions, but CT measurements are generally lower than reported tissue measurements	
2013	Hayashi et al. ⁷⁷	51 (all AA undergoing ablation, CV, and NCV)	0.67 mm slice thickness	Pericardial fat excluded on basis of HU. LAWT measured in 11 distinct locations. Multiplanar reconstructions taken to measure LAWT (oblique coronal to parallel to posterior wall or superior PV for LA, roof, oblique axial perpendicular to LA posterior wall to measure mid posterior and infero-posterior walls, axial plane at level of mitral isthmus to measure MI and oblique reconstructed image perpendicular to sup LLR to measure LLR LAWT)	11 locations—right (R), middle (M), and left (L) of each of roof, mid posterior (mid post) and infero-posterior (inf-post) wall, then LLR and mitral isthmus	HCM R roof M roof L roof R M post mid L mid post R inf-post M inf-post mid L inf-post MI LLR 1.93 ± 0.49 2.20 ± 0.51 1.96 ± 0.34 1.90 ± 0.42 1.44 ± 0.17 1.85 ± 0.35 1.66 ± 0.20 1.64 ± 0.25 1.62 ± 0.16 2.38 ± 0.36 2.20 ± 0.55 Control 1.95 ± 0.35 2.23 ± 0.31 1.98 ± 0.36 1.89 ± 0.21 1.58 ± 0.22 1.84 ± 0.22 1.75 ± 0.27 1.77 ± 0.20 1.747 ± 0.18 2.21 ± 0.31 2.14 ± 0.39	2 3 4 5 7	2—CT gives lower measurement on posterior wall than tissue specimens 4—CT gives lower measurement than tissue at mid posterior wall and mid infero-posterior wall (other regions no difference) 5—CT gives similar measurement mid posterior wall, higher value at MI compared with histology 7—CT measurements lower at mid posterior wall than tissue study In both groups	LA wall thinner in HCM patients compared with controls at mid posterior wall and infero-posterior wall (other regions no difference)
2014	Park et al. ⁷⁸	33 (all AA undergoing ablation)		Inner and outer borders defined (no further info) and electronic calipers measured wall thickness in 31 pre-specified locations (identified on 3D volume rendered image and multiplanar reformatted images), measurements taken on multiplanar reformatted images—choice not further defined	Grouped from 31 locations into 7 areas: LAA, roof, anterior wall, posterior wall, floor, lateral wall, septum	Site LAA Roof Ant Post Floor Septum Median ± SD 2.2 ± 0.6 2.0 ± 0.6 1.8 ± 0.3 1.7 ± 0.3 1.7 ± 0.3 1.8 ± 0.4 2.4 ± 0.8	2 4 5 7	2—CT gives lower measurement on anterior, posterior and lateral wall 4—CT gives lower measurement than on posterior wall 5—CT gives similar measurements anterior wall and septum, higher measurements roof, posterior 7—CT gives lower measurement than histology	Regions with CFAE had thicker walls

2014	Wi et al. ⁵⁷	31 (all AA undergoing ablation)	Reconstructed CT with 0.75 mm slice thickness	LAWT measurements obtained in 31 pre-specified locations. Surface divided on 3D VR image, point marked in centre of each region. To measure, defined a point on LA wall on 3D VR, axial, coronal, and sagittal images (to obtain perpendicular measurements). Measurements then made semi-automatically using software to identify transition inner and outer border of LA. Five measurements taken within 5 mm of each reference point and mean calculated	Grouped from locations to give mean (\pm SD) overall, at anterior appendage base and at lateral wall	Overall mean (\pm SD)	2.4 (\pm 0.4) mm (range 1.5–3.1 mm) 3.4 (\pm 1.2) 1.5 (\pm 0.4)	2	2—CT gives lower measurements than tissue samples at lateral wall
2015	Takahashi et al. ⁶³	50 AF (29 paroxysmal, 21 persistent) 25 SR	0.5 mm slice thickness	Epicardial fat excluded by excluding voxels -50 to -200 HU. Measurements taken in coronal plane in LA roof and axial plane in other locations	LAWT thickness measurements acquired at five pre-selected locations on LA wall (anterior wall, roof and septum and posterior wall, roof and septum and LAA) and eight pre-selected locations at PV-LA junction. At each site in LA three measurements taken—within 5 mm of thickest part of LA and mean taken	LA roof Anterior wall ^a Posterior wall ^a Septum ^a LA appendage ^a	Control group 2.39 \pm 0.5 mm 1.65 \pm 0.44 mm 1.61 \pm 0.31 mm 1.17 \pm 0.29 mm 1.14 \pm 0.4 mm	AF group 2.46 \pm 0.63 mm 1.93 \pm 0.44 mm 1.93 \pm 0.4 mm 1.42 \pm 0.34 mm 1.41 \pm 0.4 mm	Significantly thicker LA wall in AF patients (a stepwise increase which followed disease status—walls thinnest in control, then paroxysmal, then persistent). Also demonstrated thicker walls in areas of dormant conduction (as exposed by ATP provocation after PVI in AF patients)
2015	Park et al. ⁶⁴	71 patients all persistent AF	0.76 mm slice thickness after reconstruction		Measurements taken at point of maximum thickness of interatrial septum 1 cm inferior to fossa ovalis. Plane not reported	Overall mean IAST	6.75 mm		
					Data grouped according to tertiles and CFAE index calculated (100 \times area deemed to represent CFAE/total LA surface area). CFAE index was compared between groups according to tertiles (significant) and using linear regression model for LA volume and LA volume index (both significant)				

NR, not reported; BI, blinded; NCV, patients without a history of cardiovascular disease; CV, patients with cardiovascular disease (excluding atrial fibrillation); AF, history of atrial fibrillation; NCM, no significant co-morbidities; SCV, structural cardiovascular changes seen at autopsy; CM, significant (non-cardiac) co-morbidities; NCD, died from non-cardiac disease; LS Ps AF, long-standing persistent AF; CAF, chronic AF (resistant to electrical or chemical cardioversion or present for > 1 year); PVI, pulmonary vein isolation.

^aOnly measured in those in whom the posterior wall came into contact with the oesophagus.

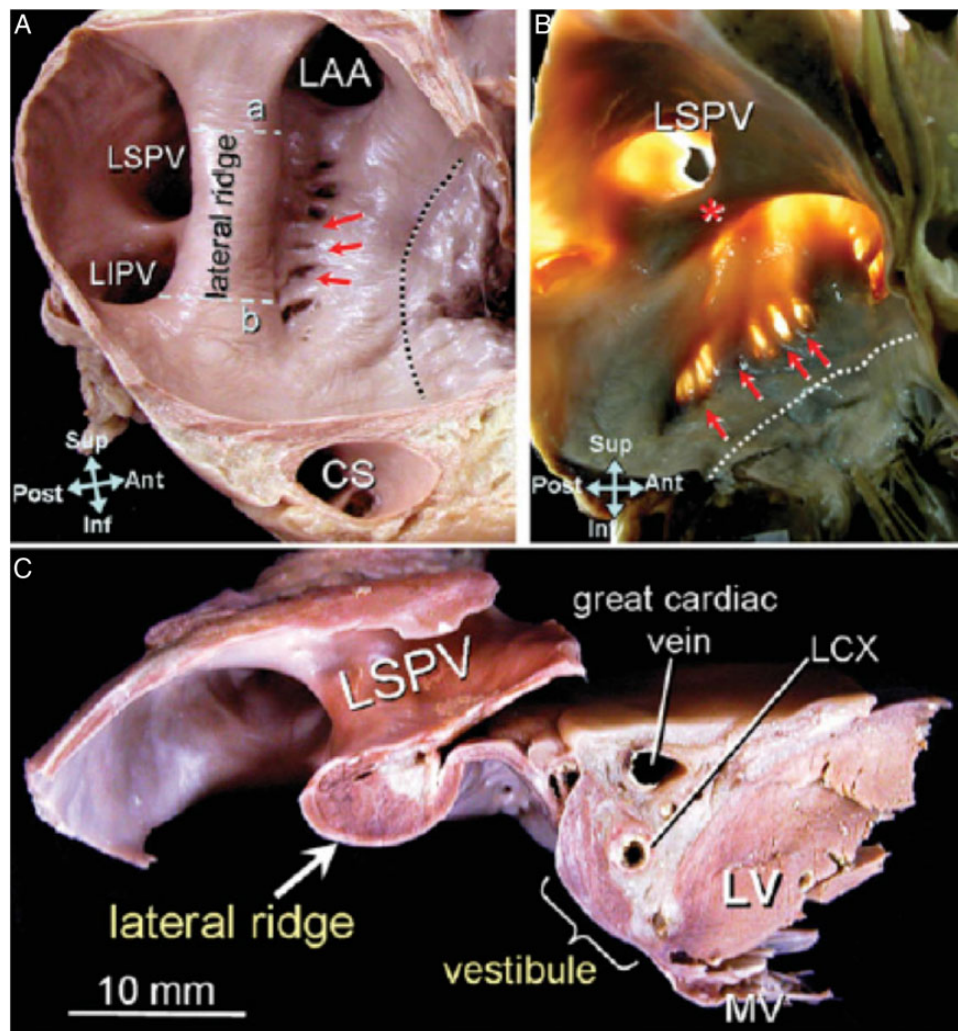


Figure 2 Tissue section of human atria reproduced with permission from Cabrera et al.⁴ (A) Endocardial surface of the left lateral wall and (B) with transillumination showing the prominent lateral ridge(*) interposed between the left atrial appendage (LAA) and the left pulmonary veins. Muscular trabeculations denoted by red arrows extend inferiorly from the ridge to the vestibule. The dotted line marks the mitral valve (MV) annulus. Lines 'a' and 'b' mark the sites where measurements were taken in this study. (C) is a section through line 'a' to demonstrate the thickness of the ridge. Also seen in the left circumflex coronary artery (LCX), coronary sinus (CS), and left ventricle (LV).

determinants of wavebreak,⁵⁴ that was often implicated in the initiation of AF. They explained this on the basis of a significant change in the source–sink relationship that a propagating wave of depolarization would meet at boundaries between thick and thin atrial wall, as previously identified in other anatomic sites⁵⁵ and *in vitro*.⁵⁶ Lines of functional conduction block have been identified during normal sinus rhythm and correlated with change in fibre geometry and wall thickness at comparable locations in the human atrium.⁵⁷

Abrupt changes in tissue thickness are also implicated in the mechanisms sustaining periods of AF.⁵⁸ In Langendorff-perfused sheep hearts, the activation sequences in normal hearts and those subjected to chronic rapid atrial pacing (RAP) were mapped optically when AF was induced. Computer-based stimulations, incorporating myocardial wall thickness, atrial stretch, and ion channel behaviour, based on the experimental results, demonstrated that transitions in

myocardial thickness stabilize 'atrial scroll waves' (ASW, three-dimensional patterns of re-entry spanning the full thickness of the myocardium⁵⁹), which may be considered as sources with the potential to drive AF.

High-density epicardial mapping of patients at cardiac surgery with AF of differing durations⁶⁰ and *in vivo* high-resolution epi- and endocardial mapping in a goat model of AF with a range of durations⁶¹ demonstrated that the degree of dissociation between the epicardial and endocardial activation increased with longer duration of AF. This work has formed the basis for a new interpretation of the multiple wavelet hypothesis, known as the 'double-layer' hypothesis. While the double-layer hypothesis proposes 'anarchical' electrical activity as the basis for fibrillation in the atrium and is therefore a fundamentally different explanation to those based on 'hierarchical' electrical activity, the dissociation of activation between the

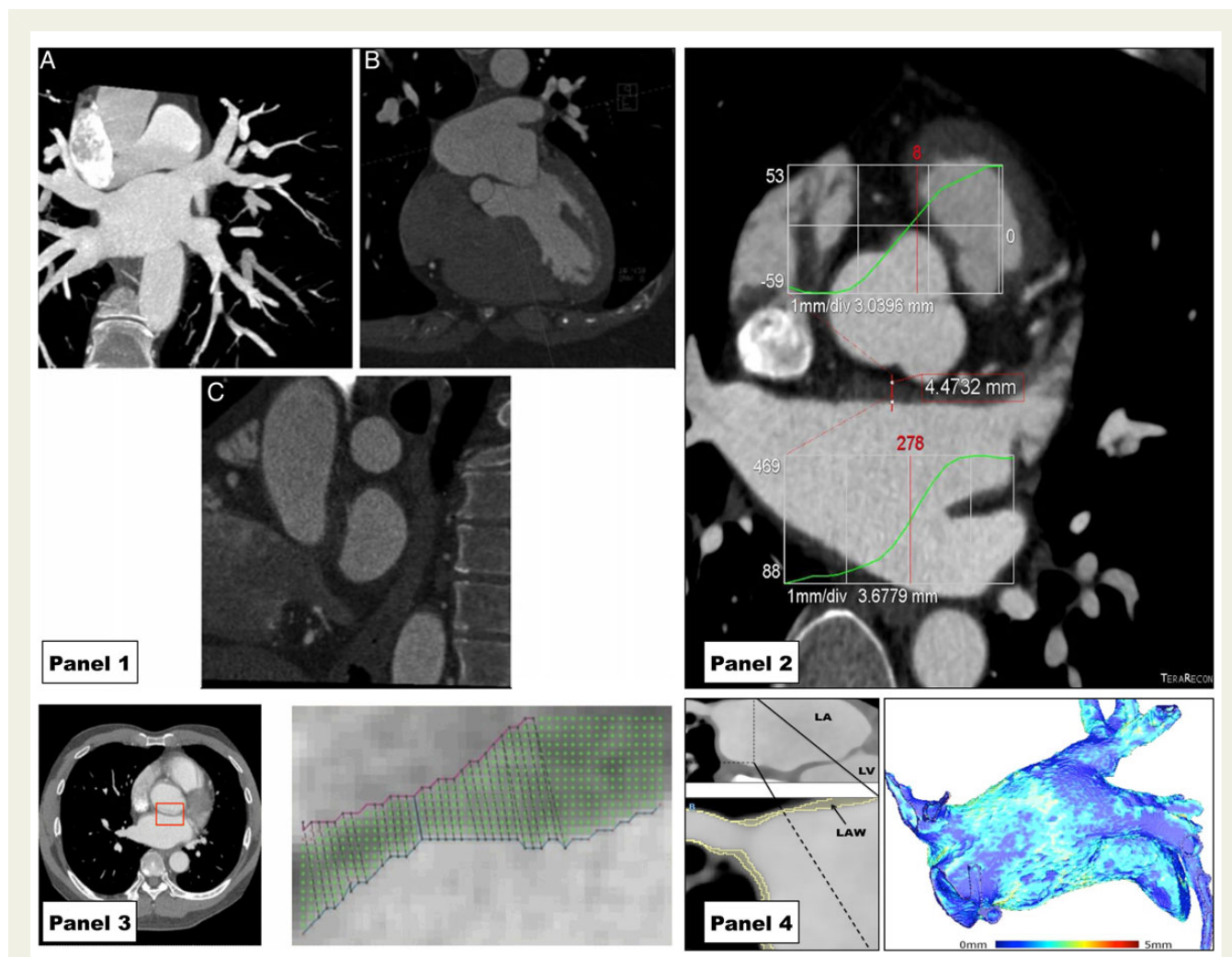


Figure 3 Recent examples of the use of cardiac CT to assess LAWT demonstrating evolving methodology. Panel 1 reproduced with permission from Beinart *et al.*³¹ Standardized planes for measuring LAWT manually. (A) Oblique coronal plane parallel to posterior wall of LA (in maximum intensity projection). (B) Axial plane perpendicular to coronal plane at the level of the mitral isthmus. (C) Sagittal plane orthogonal to the original plane near the ostium of the left pulmonary vein. Panel 2 reproduced with permission from Wi *et al.*³⁷ Semi-automatic measurement of the LAWT based on histogram intensities (projected onto CT image) after manually selecting a region containing the LA wall. Panel 3 reproduced with permission from Dewland *et al.*³⁸ An example of an automated, computer-based segmentation of the LA wall. (A) Axial plane of contrast-enhanced cardiac CT with anterior LA wall identified by red box. (B) An expanded illustration of this region with LA wall identified by computer algorithm on the basis of voxel intensity. Panel 4: a semi-automated approach to LA wall segmentation based on HU intensity that has been used to generate whole chamber LAWT maps as reported by Bishop *et al.*³⁹ Left hand image demonstrates a multiplanar-reconstructed CT image of the left atrium. Expanded region shows the LA roof and right superior pulmonary vein with LA wall as identified by computer algorithm in yellow. Right image is a visual representation of the LAWT throughout the chamber calculated using the method reported by Bishop *et al.* based on generating field lines and solving the Laplace equation.

epicardial and endocardial surfaces reinforces the concept that the three-dimensional structure of the atria will play a significant role in determining the electrical activity on which AF depends.

Recent simultaneous epi- and endocardial optical mapping study⁶² in coronary perfused *ex vivo* human right atrial specimens has demonstrated the capacity of human atrial tissue to harbour stable intramural re-entry circuits. This work is the first demonstration of the ability of human atrial tissue to harbour intramural re-entry and contributes further evidence in support of the importance of the complex atrial microstructure in determining electrophysiological behaviour.

A number of clinical studies have reported evidence suggesting atrial tissue dimensions may predict the local atrial electrophysiological behaviour in patients undergoing AF ablation. Tissue thickness as measured on CT has been correlated with the presence of complex fractionated atrial electrograms (CFAEs),³⁷ scar as defined by endocardial voltage amplitude⁶³ and proportion of endocardium in which CFAEs may be identified.⁶⁴ While the significance of CFAEs is uncertain, these studies suggest the possibility of predicting *in vivo* electrophysiological behaviour with anatomy assessed using cardiac CT (Figures 3 and 4).

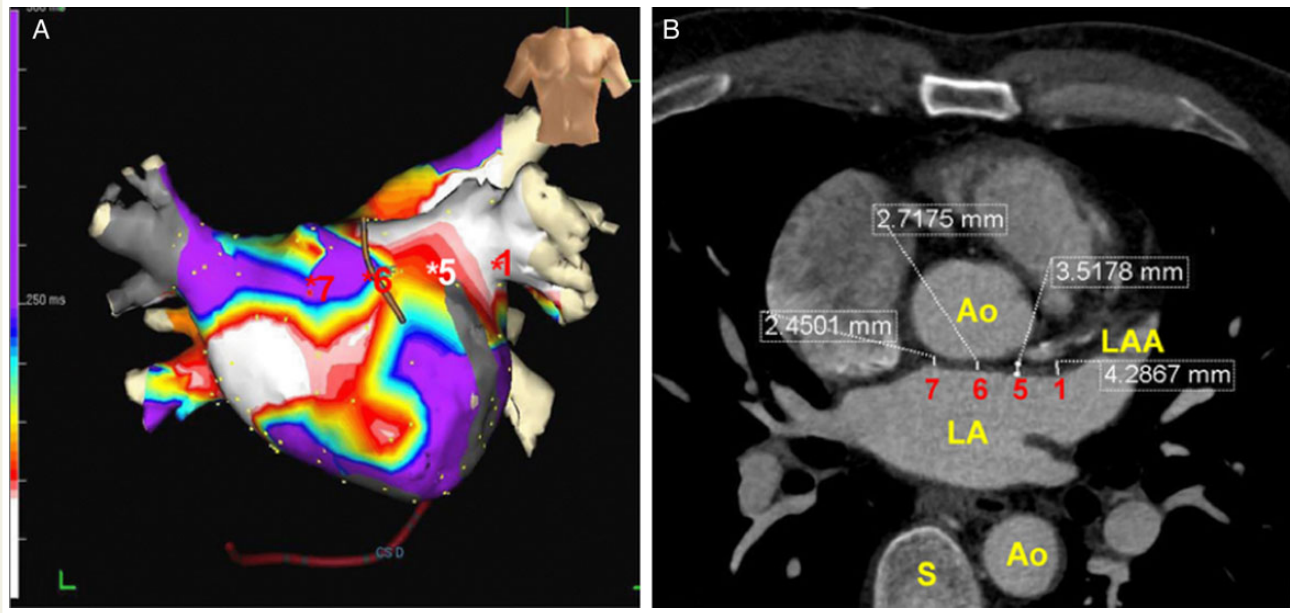


Figure 4 The correlation of CT-measured LAWT with clinically measurable electrophysiological phenomena. Reproduced with permission from Wi et al.³⁷ Left hand panel (A) is colour map representing the summation of CFAEs across the left atrium under an anteroposterior projection. On the left hand side (B) is the CT image from which LAWT measurements were made with representative measurements. In this report, CFAEs were observed more frequently in regions with increased atrial wall thickness (sites 1 and 5).

There remain many outstanding questions about the spatio-temporal organization of atrial electrical activity during human AF, but a crucial role for the three-dimensional characteristics of the tissue involved seems increasingly likely.

The impact of left atrial wall thickness on treatment: safety and efficacy considerations

Prior to invasive electrophysiology study and AF ablation, Suenari et al.⁶⁵ compared CT-determined LAWT at a range of LA and pulmonary vein locations between those who experienced a recurrence of AF and those who did not. The study identified greater wall thickness at the superior left lateral ridge (LLR, the region defined as that between the left pulmonary veins and the LA appendage) in those who experienced a recurrence of AF after a single pulmonary vein isolation procedure, while in other areas there was no difference. As well as measuring increased LAWT in AF patients when compared with controls, Takahashi et al.⁶³ found the wall of the left atrium–pulmonary vein junction to be significantly thicker at sites of adenosine-provoked pulmonary vein reconnection following pulmonary vein isolation (PVI), an observation that is consistent with failure to achieve a local transmural lesion. These studies indicate that atrial wall thickness may be a useful predictor of response to AF ablation and in the future may have a role in the prediction of response to and, ultimately, titrating delivery of, RF energy during AF ablation.

In addition to the use of CT for the assessment of LAWT, it has been used for the acute assessment of RF lesions. Girard et al.⁶⁶ demonstrated the identification of ventricular RF lesions in porcine ventricular tissue using C-arm CT. The identification of RF lesions

has been more extensively investigated using MRI^{67–69}; however, the demonstration of CT's ability to identify acute RF lesions opens up the possibility of exploiting CT's higher spatial resolution in the atria to assess these lesions acutely as well.

The incidence of a significant complication associated with a catheter ablation procedure is 4–5%.^{70,71} The most serious complications of RFCA are due to perforation of the atrial wall.^{72,73} Risk of atrial perforation during ablation is likely to depend at least partly upon LAWT. It is recognized that RF application on the posterior LA wall is associated with a greater risk of serious complications than elsewhere because of oesophageal proximity, and current guidelines recommend the use of lower energy when RF is applied here.⁷⁴ An imaging modality that could localize areas of decreased wall thickness more precisely may facilitate safer RF energy delivery. If a technique could simultaneously identify regions of increased wall thickness and it could be demonstrated that these required differential energy applications for successful transmural lesion creation, the assessment of LAWT would rapidly assume a central role by facilitating tissue tailored lesion delivery and the possibility of safety and efficacy dividends.

Conclusions

The left atrium is the critical cardiac chamber in the pathophysiology of AF, and the success of current treatments for AF is highly dependent upon the ability to create contiguous, transmural lesions. Cardiac CT is the optimal imaging modality to measure atrial wall thickness, and there has been a recent increase in the number of reports using CT for this indication. Electrophysiological behaviour

appears to change with wall thickness profile both under experimental conditions and *in vivo*. A systematic examination of the effects of changes in wall thickness on local electrophysiology *in vivo* would likely contribute to this investigation. In addition, the accurate assessment of atrial wall thickness may provide important safety information prior to the delivery of RF energy and has the potential to improve the safety of AF ablation.

Funding

The research was funded/supported by the National Institute for Health Research (NIHR) Clinical Research Facility at Guy's & St Thomas' NHS Foundation Trust and NIHR Biomedical Research Centre based at Guy's and St Thomas' NHS Foundation Trust and King's College London. This work was supported by the Medical Research Council (grant number MR/N001877/1). The views expressed are those of the author(s) and not necessarily those of the NHS, the NIHR, the MRC, or the Department of Health.

Conflict of interest: none declared.

References

- Becker AE. Left atrial isthmus: anatomic aspects relevant for linear catheter ablation procedures in humans. *J Cardiovasc Electrophysiol* 2004;**15**:809–12.
- Hall B, Jeevanantham V, Simon R, Filippone J, Vorobiof G, Daubert J. Variation in left atrial transmural wall thickness at sites commonly targeted for ablation of atrial fibrillation. *J Interv Card Electrophysiol* 2006;**17**:127–32.
- Sánchez-Quintana D, Cabrera JA, Climent V, Farré J, De Mendonça MC, Ho SY. Anatomic relations between the esophagus and left atrium and relevance for ablation of atrial fibrillation. *Circulation* 2005;**112**:1400–5.
- Cabrera JA, Ho SY, Climent V, Sánchez-Quintana D. The architecture of the left lateral atrial wall: a particular anatomic region with implications for ablation of atrial fibrillation. *Eur Heart J* 2008;**29**:356–62.
- Platonov PG, Ivanov V, Ho SY, Mitrofanova L. Left atrial posterior wall thickness in patients with and without atrial fibrillation: data from 298 consecutive autopsies. *J Cardiovasc Electrophysiol* 2008;**19**:689–92.
- Ho SYEN, Ph D, Sanchez-quintana D, Cabrera JA, Anderson RH. Anatomy of the left atrium?: implications for radiofrequency ablation of atrial fibrillation. *J Cardiovasc Electrophysiol* 1999;**10**:1525–34.
- Schwartzman D, Schoedel K, Stolz DB, Di Martino E. Morphological and mechanical examination of the atrial "intima". *Europace* 2013;**15**:1557–61.
- Wolf C, Sessler S, Boer K, Juraszek A, MacGowan F, Cowan D et al. Atrial remodeling after the fontan operation. *Am J Cardiol* 2009;**104**:1737–42.
- Sanfilippo AJ, Abascal VM, Sheehan M, Oertel LB, Harrigan P, Hughes RA et al. Atrial enlargement as a consequence of atrial fibrillation. A prospective echocardiographic study. *Circulation* 1990;**82**:792–7.
- Nishida K, Michael G, Dobrev D, Nattel S. Animal models for atrial fibrillation: clinical insights and scientific opportunities. *Europace* 2010;**12**:160–72.
- Kerr CR, Humphries KH, Talajic M, Klein GJ, Connolly SJ, Green M et al. Progression to chronic atrial fibrillation after the initial diagnosis of paroxysmal atrial fibrillation: results from the Canadian Registry of Atrial Fibrillation. *Am Heart J* 2005;**149**:489–96.
- Yoon YE, Oh I-Y, Kim S-A, Park K-H, Kim SH, Park J-H et al. Echocardiographic predictors of progression to persistent or permanent atrial fibrillation in patients with paroxysmal atrial fibrillation (E6P Study). *J Am Soc Echocardiogr* 2015;**28**:709–17.
- Tiwari S, Schirmer H, Jacobsen BK, Hopstock LA, Nyrnes A, Heggelund G et al. Association between diastolic dysfunction and future atrial fibrillation in the Tromsø Study from 1994 to 2010. *Heart* 2015;**101**:1302–8.
- López-Candales A. Is the presence of interatrial septal hypertrophy a marker for atrial fibrillation in the elderly? *Am J Geriatr Cardiol* 2002;**11**:399–403.
- López-Candales A, Grewal H, Katz W. The importance of increased interatrial septal thickness in patients with atrial fibrillation: a transesophageal echocardiographic study. *Echocardiography* 2005;**22**:408–14.
- Ren J-F, Callans DJ, Schwartzman D, Michele JJ, Marchlinski FE. Changes in local wall thickness correlate with pathological lesion size following radiofrequency catheter ablation: an intracardiac echocardiographic imaging study. *Echocardiography* 2001;**18**:503–7.
- Ren B, Mulder HW, Haak A, Van Stralen M, Szili-Torok T, Pluim JPW et al. A transoesophageal echocardiographic image acquisition protocol for wide-view fusion of three-dimensional datasets to support atrial fibrillation catheter ablation. *J Interv Card Electrophysiol* 2013;**37**:21–6.
- Morgan RB, Kwong R. Role of cardiac MRI in the assessment of cardiomyopathy. *Curr Treat Options Cardiovasc Med* 2015;**17**:53.
- McGann CJ, Kholmovski EG, Oakes RS, Blauer JJE, Daccarett M, Segerson N et al. New magnetic resonance imaging-based method for defining the extent of left atrial wall injury after the ablation of atrial fibrillation. *J Am Coll Cardiol* 2008;**52**:1263–71.
- Harrison JL, Jensen HK, Peel SA, Chiribiri A, Grondal AK, Bloch LO et al. Cardiac magnetic resonance and electroanatomical mapping of acute and chronic atrial ablation injury: a histological validation study. *Eur Heart J* 2014;**35**:1486–95.
- McGann C, Kholmovski E, Blauer J, Vijayakumar S, Haslam T, Cates J et al. Dark regions of no-reflow on late gadolinium enhancement magnetic resonance imaging result in scar formation after atrial fibrillation ablation. *J Am Coll Cardiol* 2011;**58**:177–85.
- Bisbal F, Guiu E, Cabanas-Grandío P, Berrueto A, Prat-Gonzalez S, Vidal B et al. CMR-guided approach to localize and ablate gaps in repeat AF ablation procedure. *JACC Cardiovasc Imaging* 2014;**7**:653–63.
- Bisbal F, Guiu E, Calvo N, Marin D, Berrueto A, Arbelo E et al. Left atrial sphericity: a new method to assess atrial remodeling. Impact on the outcome of atrial fibrillation ablation. *J Cardiovasc Electrophysiol* 2013;**24**:752–9.
- Bisbal F, Guiu E, Cabanas P, Calvo N, Berrueto A, Tolosana JM et al. Reversal of spherical remodeling of the left atrium after pulmonary vein isolation: incidence and predictors. *Europace* 2014;**16**:840–7.
- Hirsh BJ, Copeland-Halperin RS, Halperin JL. Fibrotic atrial cardiomyopathy, atrial fibrillation, and thromboembolism: mechanistic links and clinical inferences. *J Am Coll Cardiol* 2015;**65**:2239–51.
- Walters TE, Ellims AH, Kalman JM. The role of left atrial imaging in the management of atrial fibrillation. *Prog Cardiovasc Dis* 2015;**58**:136–51.
- Hsing J, Peters DC, Knowles BR, Manning WJ, Josephson ME. Cardiovascular magnetic resonance imaging of scar development following pulmonary vein isolation: a prospective study. *PLoS One* 2014;**9**:e104844.
- Yokokawa M, Tada H, Koyama K, Ino T, Naito S, Oshima S et al. Thickening of the left atrial wall shortly after radiofrequency ablation predicts early recurrence of atrial fibrillation. *Circ J* 2010;**74**:1538–46.
- Lemola K, Sneider M, Desjardins B, Case I, Han J, Good E et al. Computed tomographic analysis of the anatomy of the left atrium and the esophagus: implications for left atrial catheter ablation. *Circulation* 2004;**110**:3655–60.
- Hoffmeister PS, Chaudhry GM, Mendel J, Almasry I, Tahir S, Marchese T et al. Evaluation of left atrial and posterior mediastinal anatomy by multidetector helical computed tomography imaging: relevance to ablation. *J Interv Card Electrophysiol* 2007;**18**:217–23.
- Beinart R, Abbasa S, Blum A, Ferencik M, Heist K, Ruskin J et al. Left atrial wall thickness variability measured by CT scans in patients undergoing pulmonary vein isolation. *J Cardiovasc Electrophysiol* 2011;**22**:1232–6.
- Pan N-H, Tsao H-M, Chang N-C, Chen Y-J, Chen S-A. Aging dilates atrium and pulmonary veins: implications for the genesis of atrial fibrillation. *Chest* 2008;**133**:190–6.
- Wang K, Ho SY, Gibson DG, Anderson RH. Architecture of atrial musculature in humans. *Br Heart J* 1995;**73**:559–65.
- Imada M, Funabashi N, Asano M, Uehara M, Ueda M, Komuro I. Anatomical remodeling of left atria in subjects with chronic and paroxysmal atrial fibrillation evaluated by multislice computed tomography. *Int J Cardiol* 2007;**119**:384–8.
- Nakamura K, Funabashi N, Uehara M, Ueda M, Murayama T, Takaoka H et al. Left atrial wall thickness in paroxysmal atrial fibrillation by multislice-CT is initial marker of structural remodeling and predictor of transition from paroxysmal to chronic form. *Int J Cardiol* 2011;**148**:139–47.
- Gupta DK, Shah AM, Giugliano RP, Ruff CT, Antman EM, Grip LT et al. Left atrial structure and function in atrial fibrillation: ENGAGE AF-TIMI 48. *Eur Heart J* 2014;**35**:1457–65.
- Wi J, Lee H-J, Uhm J-S, Kim J-Y, Pak H-N, Lee M et al. Complex fractionated atrial electrograms related to left atrial wall thickness. *J Cardiovasc Electrophysiol* 2014;**25**:1141–9.
- Dewland TA, Wintermark M, Vaysman A, Smith L, Tong E, Eric V et al. Use of computed tomography to identify atrial fibrillation associated differences in left atrial wall thickness and density. *Pacing Clin Electrophysiology* 2014;**36**:55–62.
- Bishop M, Rajani R, Plank G, Carr-White G, Wright M, O'Neill MD et al. A novel technique to measure atrial wall thickness using cardiac computed tomography. *Europace* 2015; Accepted for publication.
- Garrey W. The nature of fibrillatory conduction of the heart: its relation to tissue mass and form. *Am J Physiol* 1914;**33**:397–414.
- Moe GK, Abildskov JA. Atrial fibrillation as a self-sustaining arrhythmia independent of focal discharge. *Am Heart J* 1959;**58**:59–70.
- Moe GK, Rheinboldt WC, Abildskov JA. A computer model of atrial fibrillation. *Am Heart J* 1964;**67**:200–20.
- Moe GK. A conceptual model of atrial fibrillation. *J Electrocardiol* 1968;**1**:145–6.

44. Allesie M, Lammers WEJP, Bonke F, Hollen J. Experimental evaluation of Moe's multiple wavelet hypothesis of atrial fibrillation. In: Zipes D, Jalife J, eds. *Cardiac Electrophysiology and Arrhythmias*. Orlando, FL: Grune and Stratton; 1985. p265–75.
45. Garrey W. Auricular fibrillation. *Physiol Rev* 1924;**4**:215–50.
46. Allesie MA, Bonke FIM, Schopman FJG. Circus movement in rabbit atrial muscle as a mechanism of tachycardia. *Circ Res* 1973;**33**:54–62.
47. Clapham DE, Lechleiter JD, Girard S. Intracellular waves observed by confocal microscopy from *Xenopus* oocytes. *Adv Second Messenger Phosphoprotein Res* 1993; **28**:161–5.
48. Lechleiter JD, John LM, Camacho P. Ca²⁺ wave dispersion and spiral wave entrainment in *Xenopus laevis* oocytes overexpressing Ca²⁺ ATPases. *Biophys Chem* 1998;**72**:123–9.
49. Byrd GD, Prasad SM, Ripplinger CM, Cassilly TR, Schuessler RB, Boineau JP et al. Importance of geometry and refractory period in sustaining atrial fibrillation: testing the critical mass hypothesis. *Circulation* 2005;**112**(Suppl.):17–13.
50. Lee AM, Aziz A, Didesch J, Clark KL, Schuessler RB, Damiano RJ. Importance of atrial surface area and refractory period in sustaining atrial fibrillation: testing the critical mass hypothesis. *J Thorac Cardiovasc Surg* 2013;**146**:593–8.
51. Wijffels MCEF, Kirchhof CJHJ, Dorland R, Allesie MA. Atrial fibrillation begets atrial fibrillation?: a study in awake chronically instrumented goats. *Circulation* 1995; **92**:1954–68.
52. Schuessler RB, Kawamoto T, Hand DE, Mitsuno M, Bromberg BI, Cox JL et al. Simultaneous epicardial and endocardial activation sequence mapping in the isolated canine right atrium. *Circulation* 1993;**88**:250–63.
53. Everett TH, Wilson EE, Hulley GS, Olgin JE. Transmural characteristics of atrial fibrillation in canine models of structural and electrical atrial remodeling assessed by simultaneous epicardial and endocardial mapping. *Heart Rhythm* 2010;**7**:506–17.
54. Klos M, Calvo D, Yamazaki M, Zlochiver S, Mironov S, Cabrera J-A et al. Atrial septopulmonary bundle of the posterior left atrium provides a substrate for atrial fibrillation initiation in a model of vagally mediated pulmonary vein tachycardia of the structurally normal heart. *Circ Arrhythm Electrophysiol* 2008;**1**:175–83.
55. Moe GK, Mendez C. Functional block in the intraventricular conduction system. *Circulation* 1971;**43**:949–54.
56. Fast VG, Klkber AG. Cardiac tissue geometry as a determinant of unidirectional conduction block: assessment of microscopic excitation spread by optical mapping in patterned cell cultures and in a computer model. *Cardiovasc Res* 1995;**29**:697–707.
57. Markides V. Characterization of left atrial activation in the intact human heart. *Circulation* 2003;**107**:733–9.
58. Yamazaki M, Mironov S, Taravanc C, Brec J, Vaquero LM, Bandaru K et al. Heterogeneous atrial wall thickness and stretch promote scroll waves anchoring during atrial fibrillation. *Cardiovasc Res* 2012;**94**:48–57.
59. Jalife J, Berenfeld O, Mansour M. Mother rotors and fibrillatory conduction?: a mechanism of atrial fibrillation. *Cardiovasc Res* 2002;**54**:204–16.
60. Allesie MA, De Groot NMS, Houben RPM, Schotten U, Boersma E, Smeets JL et al. Electropathological substrate of long-standing persistent atrial fibrillation in patients with structural heart disease longitudinal dissociation. *Circ Arrhythmia Electrophysiol* 2010;**3**:606–15.
61. Eckstein J, Zeemering S, Linz D, Maesen B, Verheule S, Van Hünnik A et al. Transmural conduction is the predominant mechanism of breakthrough during atrial fibrillation: evidence from simultaneous endo-epicardial high-density activation mapping. *Circ Arrhythmia Electrophysiol* 2013;**6**:334–41.
62. Hansen BJ, Zhao J, Csepe TA, Moore BT, Li N, Jayne LA et al. Atrial fibrillation driven by micro-anatomic intramural re-entry revealed by simultaneous sub-epicardial and sub-endocardial optical mapping in explanted human hearts. *Eur Heart J* 2015;**36**:2390–401.
63. Takahashi K, Okumura Y, Watanabe I, Nagashima K, Sonoda K, Sasaki N et al. Relation between left atrial wall thickness in patients with atrial fibrillation and intra-cardiac electrogram characteristics and ATP-provoked dormant pulmonary vein conduction. *J Cardiovasc Electrophysiol* 2015;**26**:597–605.
64. Park YM, Park HC, Ban J-E, Choi J-I, Lim HE, Park SVV et al. Interatrial septal thickness is associated with the extent of left atrial complex fractionated atrial electrograms and acute procedural outcome in patients with persistent atrial fibrillation. *Europace* 2015;**17**:1700–7.
65. Suenari K, Nakano Y, Hirai Y, Ogi H, Oda N, Makita Y et al. Left atrial thickness under the catheter ablation lines in patients with paroxysmal atrial fibrillation: insights from 64-slice multidetector computed tomography. *Heart Vessels* 2013;**28**:360–8.
66. Girard EE, Al-Ahmad A, Rosenberg J, Luong R, Moore T, Lauritsch G et al. Contrast-enhanced C-arm CT evaluation of radiofrequency ablation lesions in the left ventricle. *JACC Cardiovasc Imaging* 2011;**4**:259–68.
67. Peters DC, Wylie JV, Hauser TH, Kissinger KV, Josephson ME, Manning WJ. Detection of pulmonary vein and left atrial scar after catheter ablation with three-dimensional navigator-gated delayed enhancement MR imaging: methods: results: conclusion. *Radiology* 2007;**243**:690–5.
68. Arujuna A, Karim R, Caulfield D, Knowles B, Rhode K, Schaeffter T et al. Acute pulmonary vein isolation is achieved by a combination of reversible and irreversible atrial injury after catheter ablation: evidence from magnetic resonance imaging. *Circ Arrhythm Electrophysiol* 2012;**5**:691–700.
69. Harrison JL, Jensen HK, Peel SA, Chiribiri A, Grøndal AK, Bloch LØ et al. Cardiac magnetic resonance and electroanatomical mapping of acute and chronic atrial ablation injury: a histological validation study. *Eur Heart J* 2014;**35**:1486–95.
70. Calkins H, Reynolds MR, Spector P, Sondhi M, Xu Y, Martin A et al. Treatment of atrial fibrillation with antiarrhythmic drugs or radiofrequency ablation: two systematic literature reviews and meta-analyses. *Circ Arrhythm Electrophysiol* 2009;**2**:349–61.
71. Cappato R, Calkins H, Chen S-A, Davies W, Iesaka Y, Kalman J et al. Updated worldwide survey on the methods, efficacy, and safety of catheter ablation for human atrial fibrillation. *Circ Arrhythm Electrophysiol* 2010;**3**:32–8.
72. Cappato R, Calkins H, Chen S-A, Davies W, Iesaka Y, Kalman J et al. Prevalence and causes of fatal outcome in catheter ablation of atrial fibrillation. *J Am Coll Cardiol* 2009;**53**:1798–803.
73. Bunch TJ, Asirvatham SJ, Friedman PA, Monahan KH, Munger TM, Rea RF et al. Outcomes after cardiac perforation during radiofrequency ablation of the atrium. *J Cardiovasc Electrophysiol* 2005;**16**:1172–9.
74. Calkins H, Kuck KH, Cappato R, Brugada J, Camm AJ, Chen S-A et al. 2012 HRS/EHRA/ECAS Expert Consensus Statement on Catheter and Surgical Ablation of Atrial Fibrillation: recommendations for patient selection, procedural techniques, patient management and follow-up, definitions, endpoints, and research trial design. *Europace* 2012;**14**:528–606.
75. Hassink RJ, Aretz HT, Ruskin J, Keane D. Morphology of atrial myocardium in human pulmonary veins. *J Am Coll Cardiol* 2003;**42**:1108–14.
76. Deneke T, Khargi K, Müller KM, Lemke B, Mügge A, Laczkovics A et al. Histopathology of intraoperatively induced linear radiofrequency ablation lesions in patients with chronic atrial fibrillation. *Eur Heart J* 2005;**26**:1797–803.
77. Hayashi H, Hayashi M, Miyauchi Y, Takahashi K, Uetake S, Tsuboi I et al. Left atrial wall thickness and outcomes of catheter ablation for atrial fibrillation in patients with hypertrophic cardiomyopathy. *J Interv Card Electrophysiol* 2014;**40**:153–60.
78. Park J, Park CH, Lee H-J, Wi J, Uhm J-S, Pak H-N et al. Left atrial wall thickness rather than epicardial fat thickness is related to complex fractionated atrial electrogram. *Int J Cardiol* 2014;**172**:e411–3.